Azelaic acid potentiates TRPV3 activity as a mechanism for skin irritation

Journal of Investigative Dermatology (2026) ■, ■–■; doi:10.1016/j.jid.2026.01.022

TO THE EDITOR

Azelaic acid (AzA) is a naturally occurring dicarboxylic acid with antibacterial, anti-inflammatory, antioxidant, and skin-brightening properties, widely used in dermatology and cosmetics (Searle et al, 2022). Although generally safe, topical AzA often causes transient irritation such as burning, stinging, erythema, and itch (Feng et al, 2024). These adverse effects, although usually mild and transient, raise questions about the molecular basis of AzA-induced irritation. Sensory mediators, particularly transient receptor potential channels and mas-related G protein–coupled receptors, are plausible targets. This study explores the mechanisms of AzA-induced irritation through computational, cellular, and behavioral analyses.

To identify putative molecular targets of AzA, 2 in silico prediction tools were applied (Supplementary Figure S1a). ReverseDock (Krause et al, 2023) ranked proteins by predicted binding energy and highlighted *HRH1*, *TRPV3*, *MRGPRX3*, and *MRGPRX1* (Supplementary Figure S1b). In parallel, DrugBAN (Bai et al, 2023) assigned high interaction likelihoods to *HRH1*, *TRPV3*, *MRGPRX1*, and *MRGPRX4* (Supplementary Figure S1c). On the basis of the consensus of low binding energy and high prediction scores, *HRH1*, *TRPV3*, and *MRGPRX1* were selected for experimental follow-up (Supplementary Figure S1d).

Functional assays were then performed to assess whether AzA directly activates these candidates (Supplementary Figure S1e). Human embryonic kidney 293T cells transiently expressing HRH1, TRPV3, or MRGPRX1 were exposed to AzA, and intracellular calcium levels were monitored. AzA failed to induce calcium signals in all conditions (Supplementary Figure S1f). Screening of additional transient receptor potential channels and mas-related G protein–coupled receptor family members showed no activation (Supplementary Figure S1g and h), indicating that AzA does not function as a direct agonist.

This outcome prompted testing of AzA as a potential modulator of agonist-evoked responses (Figure 1a). Pre-incubation with AzA did not alter histamine responses in HRH1-expressing cells (Figure 1b) or BAM8-22 responses in MRGPRX1-expressing cells (Figure 1c). By contrast, AzA significantly potentiated carvacrol-evoked calcium responses in TRPV3-expressing cells (Figure 1d and e), with no effect in pcDNA controls (Figure 1f). In TRPV3-stable cell lines, potentiation was concentration dependent (Figure 1g) and was completely abolished by selective TRPV3 antagonists trpvicin (Figure 1h) and TRPV3-74a (Supplementary Figure S1i), confirming specificity.

To examine potentiation, 2-aminoethoxydiphenyl borate was tested as another TRPV3 agonist. AzA enhanced 2-aminoethoxydiphenyl borate–induced responses, demonstrating that effect beyond carvacrol (Supplementary Figure S1j and k). Because carvacrol also activates TRPA1 (Mukaiyama et al, 2020), TRPA1-expressing cells were examined; AzA failed to potentiate carvacrol-evoked responses in this context (Supplementary Figure S1l and m), confirming selectivity for TRPV3. Furthermore, buffer pH measurements after AzA incubation showed no significant acidification (7.252 ± 0.010, $n = 5$), excluding pH-mediated effects on TRPV3 (Cao et al, 2012). Collectively, AzA selectively potentiates TRPV3 activity, independent of agonist and extracellular pH.

To explore the molecular basis, docking analyses revealed carvacrol binding near TRPV3 residues Arg568, Phe441, Phe442, and Tyr565 (Supplementary Figure S2a). AzA engaged overlapping residues—Phe441, Phe442, Tyr565—albeit with a different orientation (Supplementary Figure S2b and c), suggesting facilitation rather than displacement. Site-directed mutagenesis confirmed this: TRPV3-F441A showed modest loss of potentiation, whereas TRPV3-Y565A exhibited complete loss (Supplementary Figure S2d–f). AlphaFold modeling indicated no global structural disruption in Y565A (Supplementary Figure S2g), although docking revealed altered AzA binding in this mutant, whereas carvacrol docking was preserved (Supplementary Figure S2h). These findings highlight Tyr565 as a critical residue for AzA-mediated modulation of TRPV3.

The in vivo relevance of TRPV3 potentiation by AzA was then examined in mice (Figure 2a). Intradermal AzA alone did not induce scratching, whereas carvacrol caused moderate responses. Their combined administration markedly enhances scratching bouts (Figure 2b), indicating TRPV3 potentiation, which was reduced by TRPV3 antagonist trpvicin (Figure 2c). Primary mouse keratinocytes showed similar potentiation, with AzA enhancing carvacrol-evoked TRPV3 responses in a concentration-dependent manner (Figure 2d and e). Five-day intradermal AzA treatment (Supplementary Figure S3a) caused mild skin lesions without altering epidermal thickness but led to increased scratching on day 5 (Supplementary Figure S3b–h). Keratinocytes isolated from treated mice exhibited elevated carvacrol responses, suppressed by trpvicin, confirming TRPV3 involvement (Figure 2f and g).

Gene and protein expression analysis further clarified these effects. *Trpv3*

Abbreviations: AzA, azelaic acid; FPP, farnesyl pyrophosphate

Accepted manuscript published online XXX; corrected proof published online XXX

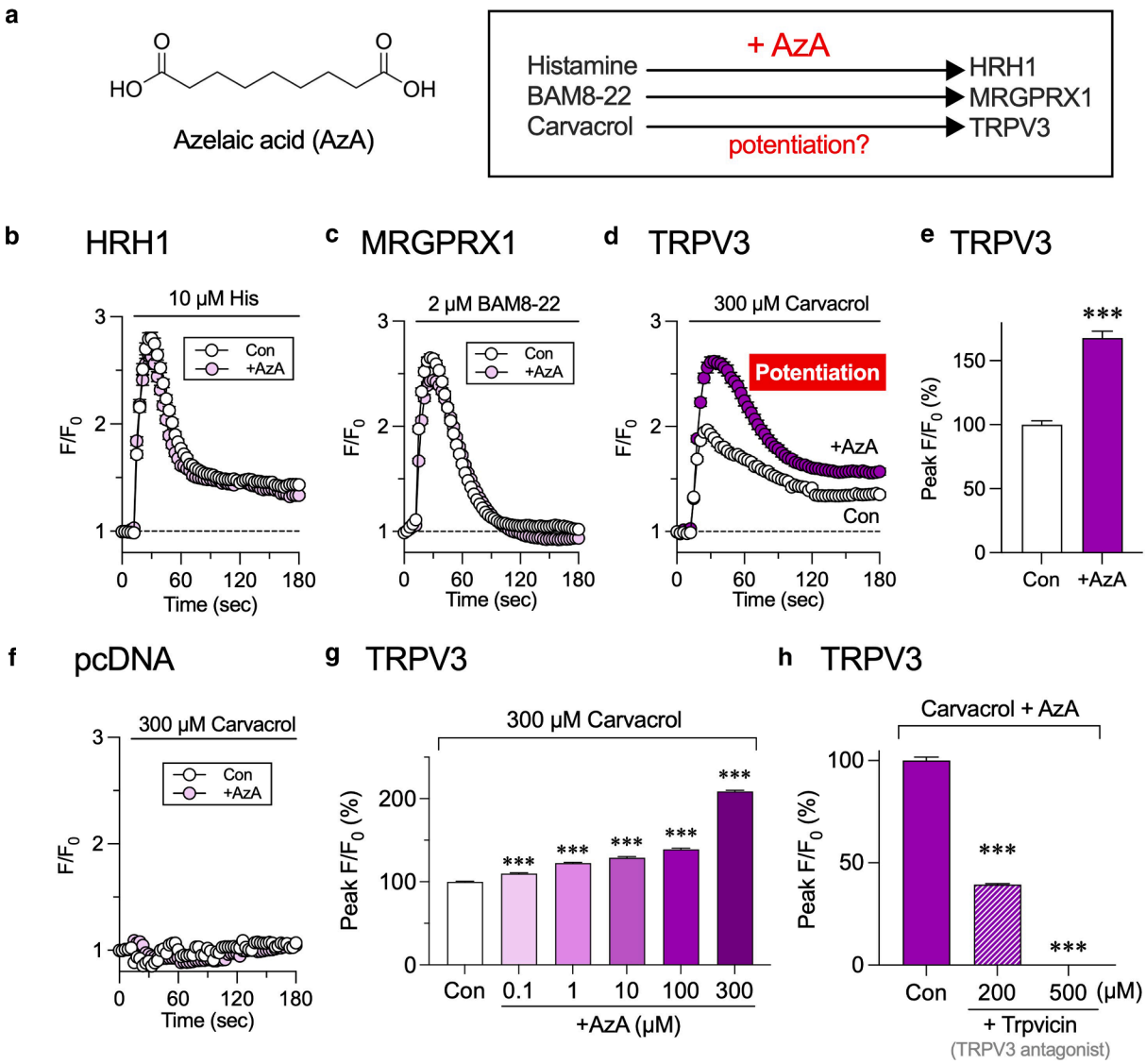

Figure 1. AzA selectively potentiates TRPV3 activity. (**a**) Experimental scheme testing whether AzA potentiates receptor responses to their agonists. (**b**) In HRH1-expressing cells, AzA did not alter histamine-induced calcium increases (n = 2133 vs 2002). (**c**) In MRGPRX1-expressing cells, AzA did not affect BAM8-22–evoked responses (n = 2007 vs 2272). (**d**) In TRPV3-expressing cells, the response to 300 μM carvacrol (n = 1171) was significantly potentiated by 100 μM AzA. (**e**) Quantification confirmed enhanced TRPV3 responses with AzA (n = 1123 vs 1171). (**f**) Carvacrol failed to induce calcium changes in mock vector (pcDNA)–transfected cells with or without AzA (n = 1235 vs 987). (**g**) AzA potentiated TRPV3 activity in a dose-dependent manner (0.1–300 μM) in the presence of 300 μM carvacrol (n = 3691, 4304, 1629, 2405, and 5956) compared with the control (n = 13,614). (**h**) The potentiating effect of AzA was blocked by the TRPV3-specific antagonist trpvicin in a dose-dependent manner (n = 2306 and 787) compared with the control (n = 2659). ***$P < .001$. AzA, azelaic acid; sec, second.

mRNA was significantly upregulated in AzA-treated skin (Supplementary Figure S3i), whereas *Tmem79*, a negative regulator of TRPV3 (Lei et al, 2023), was reduced (Supplementary Figure S3j). Immunostaining confirmed increased TRPV3 protein, abolished by blocking peptide control (Supplementary Figure S3k and l). These results demonstrate that repeated AzA exposure drives the upregulation of TRPV3 at both transcript and protein levels, contributing to sensitization and irritation development.

Because AzA acts as a potentiator rather than an agonist, an endogenous TRPV3 activator was considered. Farnesyl pyrophosphate (FPP), a known TRPV3 agonist (Supplementary Figure S4a) (Bang et al, 2010), was potentiated by AzA in TRPV3-expressing cells (Supplementary Figure S4b and c). *Fdps* mRNA, encoding the enzyme responsible for FPP synthesis (Supplementary Figure S4d), was upregulated in AzA-treated skin (Supplementary Figure S4e), suggesting enhanced endogenous production. Docking revealed adjacent, nonoverlapping binding sites for AzA and FPP (Supplementary Figure S4f), supporting cooperative interaction. These findings indicate that AzA amplifies TRPV3 signaling by potentiating FPP-induced activation and promoting FPP biosynthesis endogenously.

Finally, human relevance was evaluated using HaCaT keratinocytes. AzA potentiated carvacrol-evoked calcium responses (Figure 2h and i), which were blocked by trpvicin (Figure 2j and k) and TRPV3-74a (Supplementary Figure S4g). AzA also enhanced

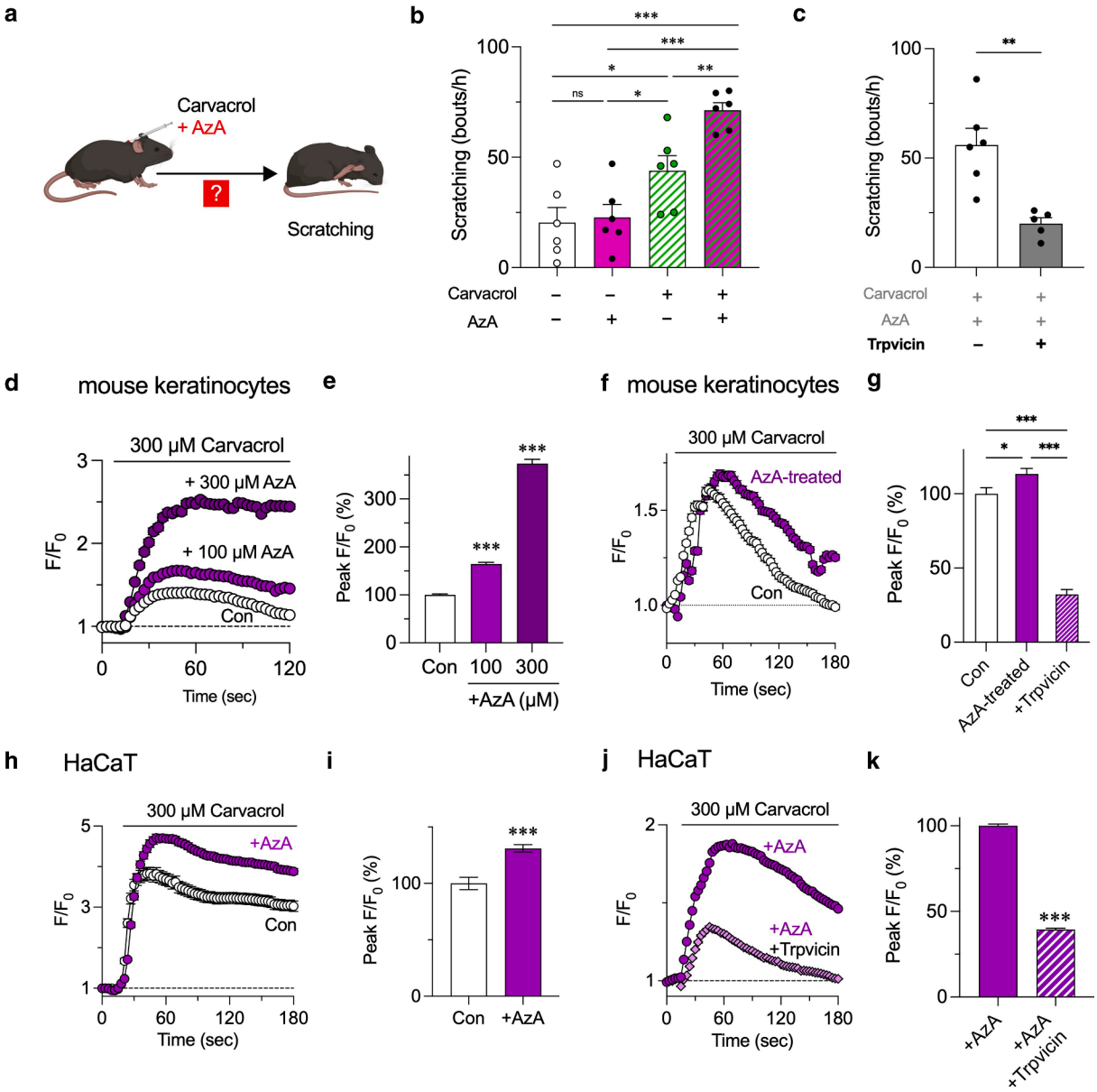

Figure 2. AzA potentiates TRPV3-mediated scratching behavior and calcium responses in keratinocytes. (**a**) Experimental scheme to evaluate whether AzA enhances carvacrol-induced scratching in mice. (**b**) Quantification of scratching bouts per hour after intradermal injection of vehicle, AzA, carvacrol, or AzA with carvacrol; coinjection significantly increased scratching compared with individual treatments. (**c**) Scratching bouts induced by the combination of carvacrol and AzA were significantly reduced by trpvicin treatment (n = 5−6 mice). (**d**) Calcium imaging traces from primary keratinocytes showing enhanced carvacrol responses with 100 or 300 μM AzA. (**e**) Quantification of peak responses confirming dose-dependent potentiation (n = 1821, 1210 vs 1912). (**f, g**) Carvacrol responses potentiated by AzA were suppressed by trpvicin (n = 1047 AzA, 1066 + trpvicin, 965 control). (**h**) Calcium traces from HaCaT cells showing enhanced carvacrol responses after 100 μM AzA pretreatment. (**i**) Quantification confirming significant potentiation (n = 591 vs 173). (**j**) AzA-induced potentiation was inhibited by trpvicin. (**k**) Quantification confirming suppression (n = 1524 vs 839). $*P < .05$, $**P < .01$, and $***P < .001$. AzA, azelaic acid; ns, not significant; sec, second.

FPP-evoked TRPV3 activity in HaCaT cells (Supplementary Figure S4h and i). These results demonstrate that AzA potentiates TRPV3-mediated responses in human keratinocytes, consistent with murine data.

This study identifies a mechanism through which AzA induces skin irritation. In silico analyses suggested HRH1, MRGPRX1, and TRPV3 as potential targets, but functional assays showed no direct activation by AzA. Instead, AzA selectively potentiates TRPV3 activity, requiring Tyr565, and enhances responses to both exogenous (carvacrol, 2-aminoethoxydiphenyl borate) and endogenous (FPP) agonists. Repeated AzA exposure in mice increased TRPV3 expression, sensitized keratinocytes, and produced skin irritation. Importantly, TRPV3 potentiation by AzA was also demonstrated in human HaCaT keratinocytes, supporting translational relevance. Although FPP upregulation and TRPV3 overexpression likely contribute to these effects, the involvement of other endogenous mediators cannot be excluded. The reliance on murine models represents a limitation, but

consistency across human keratinocytes strengthens the conclusion. These findings suggest that AzA-induced irritation arises from TRPV3 potentiation and highlight TRPV3 antagonists as potential therapeutic agents for mitigating AzA-related and broader TRPV3-mediated skin irritation.

ETHICS STATEMENT

All animal procedures were reviewed and approved by the Institutional Animal Care and Use Committee of Gachon University (approval number GU1-2023-IA0026), and all experiments were conducted in compliance with the university's animal care guidelines.

DATA AVAILABILITY STATEMENT

Data will be made available by the corresponding author upon reasonable request.

KEYWORDS

Calcium imaging; Ion channel modulation; Itch; Keratinocytes; Molecular docking

ORCIDs

Diwas Rawal: http://orcid.org/0009-0005-9152-2158
Wook-Joo Lee: http://orcid.org/0000-0002-3676-0170
Won-Sik Shim: http://orcid.org/0000-0002-1020-685X

CONFLICT OF INTEREST

The authors state no conflicts of interest.

ACKNOWLEDGMENTS

This study was supported by a grant from the National Research Foundation of Korea funded by the Korean government (Ministry of Science and ICT) (RS-2024-00333509); a grant of the Korea Health Technology R&D Project through the Korea Health Industry Development Institute, funded by the Ministry of Health & Welfare, Republic of Korea (RS-2025-02217860); and the Gachon University Research Fund (number 202300460001, Republic of Korea).

AUTHOR CONTRIBUTIONS

Conceptualization: W-SS; Funding Acquisition: W-SS; Investigation: DR, W-JL; Methodology: DR; Project Administration: W-SS; Software: DR; Supervision: W-SS; Validation: W-JL; Writing — Original Draft Preparation: DR; Writing — Review and Editing: W-SS

***Diwas Rawal*[1,2], *Wook-Joo Lee*[1,2] and *Won-Sik Shim*[1,2,*]**

[1]*College of Pharmacy, Gachon University, Incheon, Republic of Korea; and* [2]*Gachon Institute of Pharmaceutical Sciences, Incheon, Republic of Korea*
[*]*Corresponding author e-mail: wsshim@gachon.ac.kr*

SUPPLEMENTARY MATERIAL

Supplementary material is linked to the online version of the paper at www.jidonline.org, and at 10.1016/j.jid.2026.01.022.

REFERENCES

Bai P, Miljković F, John B, Lu H. Interpretable bilinear attention network with domain adaptation improves drug-target prediction. Nat Mach Intell 2023;5:126–36.

Bang S, Yoo S, Yang TJ, Cho H, Hwang SW. Farnesyl pyrophosphate is a novel pain-producing molecule via specific activation of TRPV3. J Biol Chem 2010;285:19362–71.

Cao X, Yang F, Zheng J, Wang K. Intracellular proton-mediated activation of TRPV3 channels accounts for the exfoliation effect of α-hydroxyl acids on keratinocytes. J Biol Chem 2012;287:25905–16.

Feng X, Shang J, Gu Z, Gong J, Chen Y, Liu Y. Azelaic acid: mechanisms of action and clinical applications. Clin Cosmet Investig Dermatol 2024;17:2359–71.

Krause F, Voigt K, Di Ventura B, Öztürk MA. ReverseDock: a web server for blind docking of a single ligand to multiple protein targets using AutoDock Vina. Front Mol Biosci 2023;10:1243970.

Lei J, Yoshimoto RU, Matsui T, Amagai M, Kido MA, Tominaga M. Involvement of skin TRPV3 in temperature detection regulated by TMEM79 in mice. Nat Commun 2023;14:4104.

Mukaiyama M, Usui T, Nagumo Y. Non-electrophilic TRPA1 agonists, menthol, carvacrol and clotrimazole, open epithelial tight junctions via TRPA1 activation. J Biochem 2020;168:407–15.

Searle T, Ali FR, Al-Niaimi F. The versatility of azelaic acid in dermatology. J Dermatolog Treat 2022;33:722–32.

SUPPLEMENTARY MATERIALS AND METHODS

Reagents

Azelaic acid (AzA) (246379), carvacrol (282197), 2-aminoethoxydiphenyl borate (100065), trpvicin (SML3758), Dispase II (D4693), G418 disulfate (A1720), and farnesyl pyrophosphate (F6892) were purchased from Sigma-Aldrich (St. Louis, MO). TRPV3-74a (6831) was from Tocris Bioscience (Bristol, United Kingdom). DMEM, EpiLife, fetal bovine serum (FBS), and Human Keratinocyte Growth Supplement were obtained from Gibco Thermo Fisher (New York, NY).

Genes

Coding sequences of the following cDNAs—*HRH1*, *TRPV1*, *TRPV2*, *Trpv3*, *TRPV4*, *Trpa1*, *Trpm1*, *Trpm3*, *MRGPRX1*, *MRGPRX2*, *MRGPRX3*, *MRGPRX4*, *Mrgpra1*, *Mrgpra3*, *Mrgprc11*, and *Mrgprb2*—were subcloned into the expression vector pcDNA3.1. All sequences showed 100% identity to the National Center for Biotechnology Information RefSeq database.

Site-directed mutagenesis of TRPV3

A site-specific mutation was introduced into the mouse *Trpv3* gene using primers designed according to standard mutagenesis protocols. The mutagenesis procedure was carried out with a commercial site-directed mutagenesis kit (Muta-Direct; iNtRON Biotechnology, Seoul, Korea), following the manufacturer's instructions. Successful incorporation of the desired mutation was verified by DNA sequencing.

Cell culture and transfection

Human embryonic kidney 293T cells (passage number 18-25) and human keratinocyte-derived HaCaT cell lines (passage number 15-22) were cultured in DMEM supplemented with 10% FBS and 1X antibiotic-antimycotic solution (100X stock), which contains penicillin G, streptomycin, and amphotericin B (AA-001; SolBio, Gyeonggido, Korea). The cells were incubated at 37 °C and 5% carbon dioxide. For transient gene expression, cells were transfected with FuGENE HD transfection reagent (Promega, Madison, WI), following the manufacturer's instructions, using a 1:3 ratio of cDNA to reagent. Calcium imaging experiments were performed 24 hours after transfection.

Establishment of a stable human embryonic kidney 293 cell line expressing TRPV3

To generate a stable TRPV3-expressing cell line, human embryonic kidney 293 cells (passage 7) were transfected with *Trpv3* subcloned into pcDNA3.1 using FuGENE 4K (Promega). After 24 hours, cells were selected with 500 μg/ml G418, refreshed every 48 hours, and maintained for 14 days. Surviving cells were subjected to limiting dilution (2−5 cells/ml) in 35-mm dishes to isolate single clones. Clones with stable growth and high TRPV3 expression were expanded and designated as the TRPV3-HEK293 cell line.

Calcium imaging

Intracellular calcium dynamics were measured using Fluo-4/AM (5 μM, Invitrogen) with 0.1% Pluronic F-127 in NBS (140 mM sodium chloride, 5 mM potassium chloride, 2 mM calcium chloride/EDTA, 0.5 mM magnesium chloride, 10 mM glucose, 5.5 mM 4-[2-hydroxyethyl]-1-piperazineethanesulfonic acid, pH 7.4). Cells were loaded for 40 minutes at 37 °C, and time-lapse images were acquired on a Leica DMi8 inverted microscope (Ex 488 nm/Em 515 nm). Calcium responses were expressed as F/F_0, where F is fluorescence at a given time, and F_0 is the baseline before treatment. Image analysis was performed in ImageJ with macros for region of interest selection and F/F_0 calculation. n values represent total cell counts from at least 3 independent experiments.

Animals and scratching behavior analysis

Male C57BL/6 mice aged 7−10 weeks (25−30 g) were obtained from Koatech (Pyeongtaek, Gyeonggi-do, Korea). Prior to behavioral testing, mice were acclimated for 30 minutes. Test compounds were dissolved in either saline or 10% DMSO and administered through intradermal injection. Carvacrol (1%) and AzA (25 μg/site in 50 μl) were delivered intradermally. For AzA-treated mouse models, animals received daily intradermal injections of AzA (25 μg/site in 50 μl) for 5 consecutive days. Trpvicin (300 μM/site in 50 μl) was intradermally pretreated into the nape of mice 15 minutes prior to carvacrol and AzA treatment. Scratching behavior was recorded for 60 minutes after injection using a video camera. A scratching bout was defined as a continuous scratching episode initiated when the hind paw left the ground and ending when it returned. The number of scratching bouts was quantified using DeepEthogram software (Bohnslav et al, 2021).

Primary culture of mice keratinocytes from adult tail skin

Keratinocytes were isolated from C57BL/6 mice aged 7−10 weeks as described (Li et al, 2017). Tail skin was obtained by longitudinal incision, and dorsal skin was obtained by excision from control or AzA-treated mice, followed by overnight incubation in Dispase buffer (4 mg/ml in EpiLife medium). Epidermis was separated, and cells were filtered (100 μm) and centrifuged (180*g*, 5 minutes). Pellets were resuspended in EpiLife medium supplemented with 1% human keratinocyte growth supplement, 10% FBS, and 1% penicillin-streptomycin and seeded at 1×10^4 cells/cm^2 in keratinocyte-specific 8-well plates. Cultures were maintained at 37 °C and 5% carbon dioxide, with medium changed every 2 days for 1 week.

RT-qPCR

Total RNA was extracted from mouse dorsal skin using an RNA extraction kit (iNtRON Biotechnology). First-strand cDNA was synthesized from the isolated RNA using the PrimeScript 1st Strand cDNA Synthesis Kit (TaKaRa, Shiga, Japan). RT-qPCR was performed on a QuantStudio 1 qPCR System (Thermo Fisher Scientific) using TB Green Premix ExTaq II (TaKaRa) with 100 ng of cDNA per reaction. Thermal cycling conditions included an initial denaturation at 95 °C for 30 seconds, followed by 40 cycles of 95 °C for 5 seconds and 60 °C for 30 seconds, with a final dissociation step to verify specificity. Gene expression levels were normalized to *Gapdh* as the internal control.

Immunohistochemistry

Mouse skin cryosections were fixed in 4% paraformaldehyde (10 minutes), treated with 0.1% sodium hydroxide/1% hydrogen peroxide (20 minutes), and incubated with 0.3% glycine (10

minutes). After PBS washes, sections were blocked for 1 hour (0.3% Triton X-100, 1% FBS) and incubated overnight at 4 °C with rabbit anti-TRPV3 antibody (1:200, Alomone, ACC-033) with synthetic peptide control (BLP-CC033). Secondary labeling was performed with Alexa Fluor 488—conjugated goat anti-rabbit IgG (1:1000, Abcam, ab150077) and DAPI (300 nM, 2 hours). Antibodies were diluted in 0.5% FBS/0.3% Triton X-100. Slides were mounted in Vectashield and imaged with a Leica DMi8 inverted fluorescence microscope.

In silico prediction of molecular interactions and structure

For ReverseDock analysis, UniProt identifications of itch-related channels and receptors were retrieved from the AlphaFold Protein Structure Database, and the AzA structure was obtained from PubChem, converted to mol2 using Open Babel (version 3.1.1), and docked with target proteins through the ReverseDock server (Krause et al, 2023). Predicted binding energies were recorded for target evaluation.

For DrugBAN analysis, the SMILES of AzA was retrieved from PubChem, and protein binding data were obtained from BindingDB and IUPHAR to expand the training set. The DrugBAN algorithm (Bai et al, 2023) was applied using AzA SMILES and target protein sequences, with confidence scores >0.8 considered positive predictions.

For molecular docking, the 3-dimensional structure of mouse TRPV3 (PDB identification: 6DVY) was downloaded from the PDB, and ligand structures (AzA, carvacrol, farnesyl pyrophosphate) were downloaded from PubChem. Proteins were processed by DockPrep, and ligands were processed by adding hydrogens and Gasteiger charges. Docking simulations with AutoDock Vina identified optimal poses on the basis of binding affinities, which were visualized in UCSF Chimera (version 1.12).

For mutant modeling, Y565 in TRPV3 was replaced with alanine in the FASTA sequence, and the Y565A-TRPV3 3-dimensional structure was predicted using AlphaFold (Abramson et al, 2024).

Statistical analysis

Data are expressed as means ± SEM. Statistical analyses were performed using GraphPad Prism (version 10). Comparisons between 2 groups were assessed using unpaired *t*-tests. For comparisons among 3 or more groups, 1-way ANOVA followed by Dunnett's or Tukey's multiple comparison tests was applied. Fisher's exact test was used to analyze differences in the proportion of responsive dorsal root ganglion neurons. A $P < .05$ was considered statistically significant for all analyses.

SUPPLEMENTARY REFERENCES

Abramson J, Adler J, Dunger J, Evans R, Green T, Pritzel A, et al. Accurate structure prediction of biomolecular interactions with AlphaFold 3. Nature 2024;630:493—500.

Bai P, Miljković F, John B, Lu H. Interpretable bilinear attention network with domain adaptation improves drug-target prediction. Nat Mach Intell 2023;5:126—36.

Bohnslav JP, Wimalasena NK, Clausing KJ, Dai YY, Yarmolinsky DA, Cruz T, et al. DeepEthogram, a machine learning pipeline for supervised behavior classification from raw pixels. eLife 2021;10:e63377.

Krause F, Voigt K, Di Ventura B, Öztürk MA. ReverseDock: a web server for blind docking of a single ligand to multiple protein targets using AutoDock Vina. Front Mol Biosci 2023;10:1243970.

Li F, Adase CA, Zhang LJ. Isolation and culture of primary mouse keratinocytes from neonatal and adult mouse skin. J Vis Exp 2017;125:e56027.

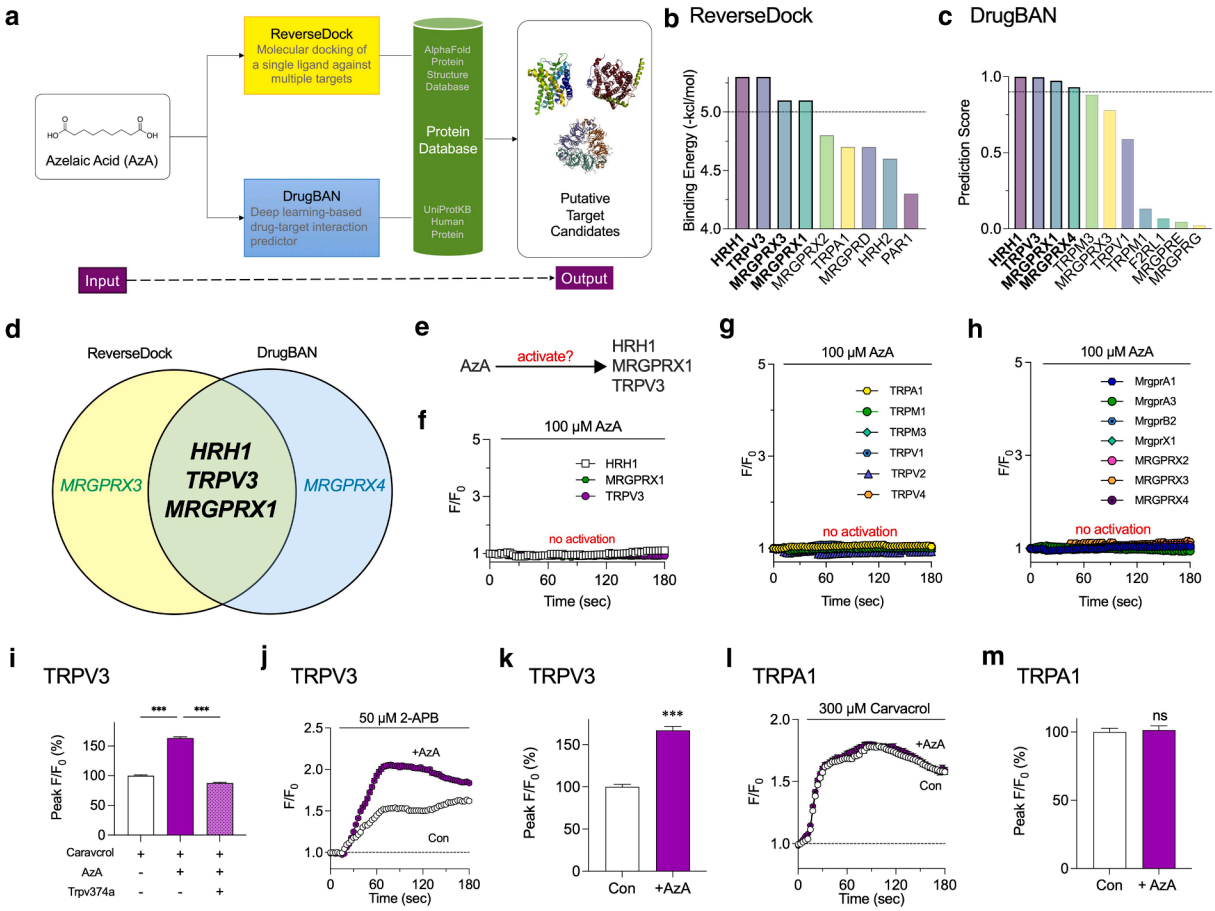

Supplementary Figure S1. (**a**) Target prediction workflow: AzA was analyzed using 2 computational tools—ReverseDock, which docks a ligand against multiple AlphaFold-predicted/UniProtKB proteins, and DrugBAN, a deep learning–based drug–target interaction predictor. (**b**) ReverseDock results showing binding energies (kcal/mol) of AzA to top-ranked proteins (lower energy = higher affinity). (**c**) DrugBAN prediction scores for AzA–target interactions (higher score = stronger probability). (**d**) Venn diagram showing overlap of targets from both tools; HRH1, TRPV3, and MRGPRX1 were predicted by both. (**e**) Schematic hypothesis that AzA may activate HRH1, MRGPRX1, or TRPV3. (**f**) Calcium imaging traces showing that 100 µM AzA did not activate HRH1-, MRGPRX1-, or TRPV3-expressing cells (n = 2194, 1232, 1362). (**g**) Calcium imaging of cells expressing TRPA1, TRPM1, TRPM3, TRPV1, TRPV2, or TRPV4 showed no response to AzA (n = 897, 1324, 1146, 975, 639, 1185). (**h**) Cells expressing MrgprA1, MrgprA3, MrgprB2, MrgprX1, MRGPRX2, MRGPRX3, or MRGPRX4 also showed no activation (n = 961, 793, 1130, 1106, 1098, 832, 1214). (**i**) AzA-mediated potentiation of TRPV3 activity was reduced by TRPV3 antagonist TRPV3-74a (+AzA, n = 1815; AzA + TRPV3-74a, n = 1269; control, n = 1950). (**j**) AzA potentiated TRPV3 activation by 2-APB (50 µM). (**k**) Quantification of 2-APB responses showing significant enhancement by AzA (n = 1674) versus control (n = 1973). (**l, m**) TRPA1 responses to carvacrol (300 µM) were unaffected by AzA, as shown by traces and quantification (n = 1996 vs n = 2101). ***$P < .001$. 2-APB, 2-aminoethoxydiphenyl borate; AzA, azelaic acid; ns, not significant.

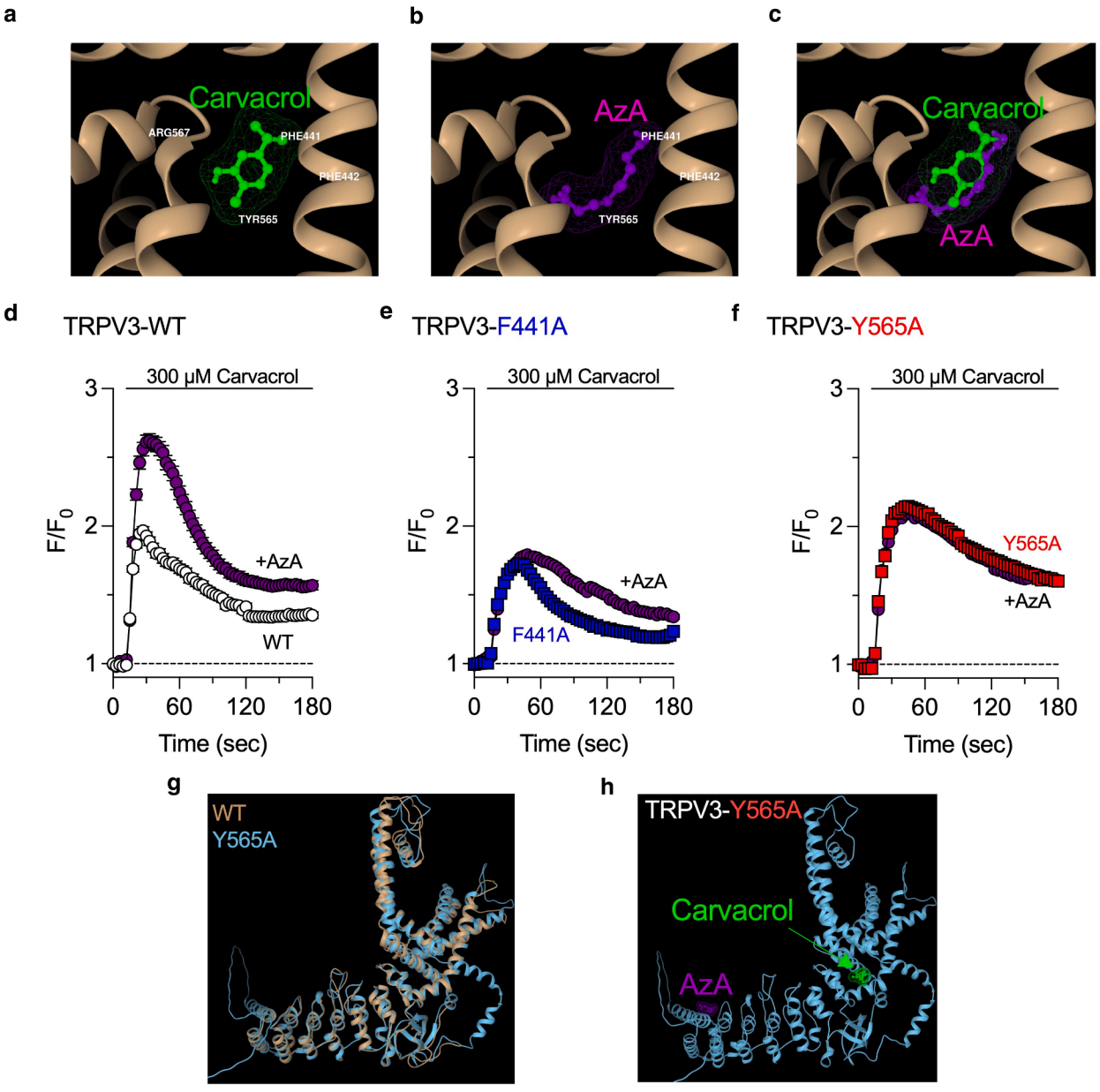

Supplementary Figure S2. (**a**) Molecular docking showing carvacrol binding to TRPV3 at Phe441, Phe442, Tyr565, and Arg567. (**b**) Docking model of AzA showing binding at a similar site, involving Phe441, Phe442, and Tyr565. (**c**) Superimposed models of carvacrol and AzA indicating overlapping binding regions on TRPV3. (**d**) Calcium imaging showing that AzA significantly potentiates carvacrol-induced responses in WT TRPV3-expressing cells (n = 1123 vs 1171). (**e**) TRPV3-F441A mutant exhibits only a modest increase in response with AzA (n = 1720 vs 1433). (**f**) TRPV3-Y565A mutant shows no AzA-mediated potentiation, indicating that Tyr565 is essential for AzA modulation (n = 2523 vs 2351). (**g**) AlphaFold-predicted structures of WT and Y565A-mutant TRPV3 show no major conformational differences. (**h**) Docking model of TRPV3-Y565A illustrating spatial separation of carvacrol and AzA. *$P < .05$, **$P < .01$, and ***$P < .001$. AzA, azelaic acid; ns, not significant; sec, second; WT, wild-type.

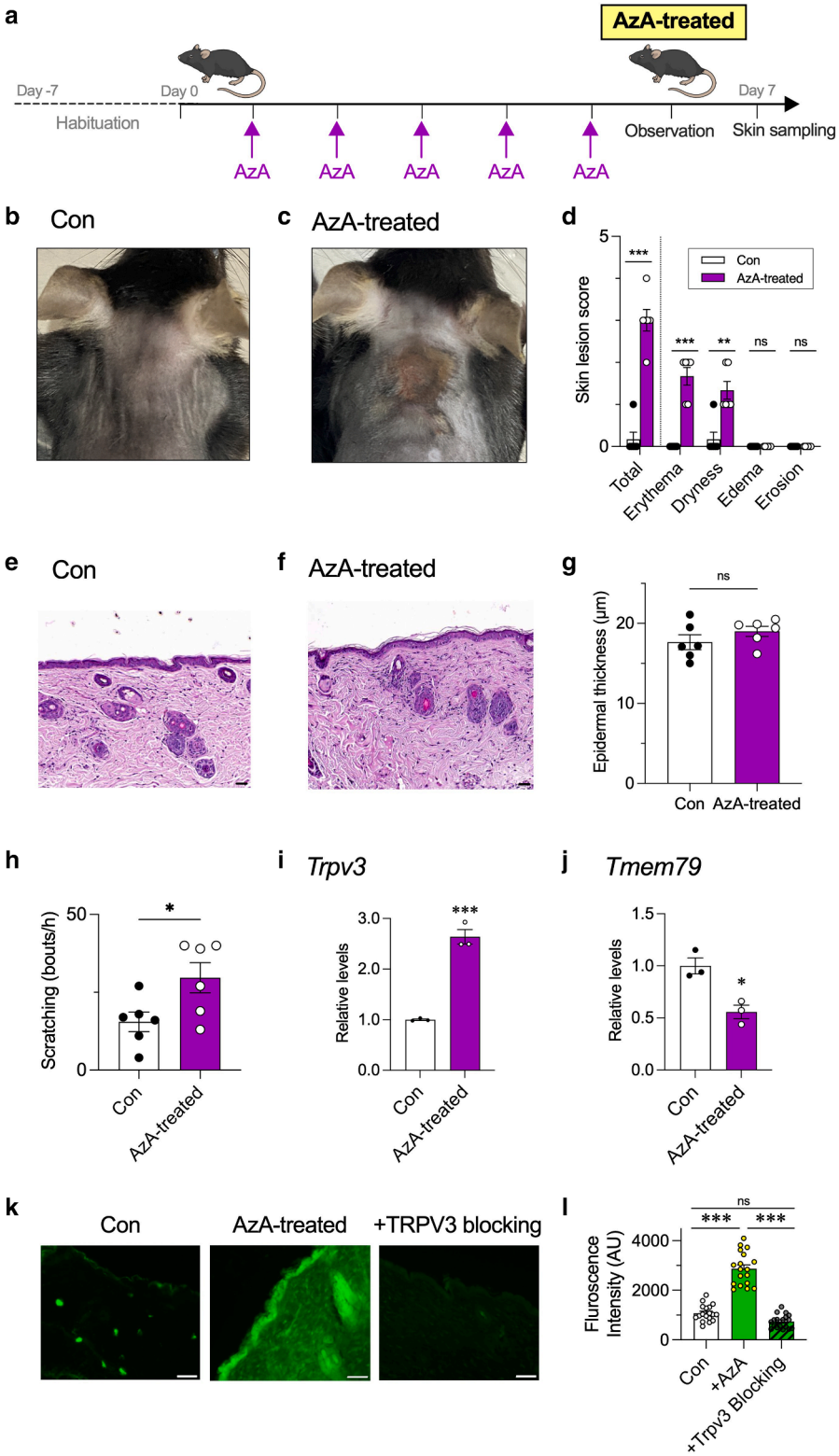

Supplementary Figure S3. (**a**) Experimental timeline: mice received daily intradermal AzA injections for 5 days, with sampling on day 7. (**b, c**) Representative dorsal skin images from (**b**) control and (**c**) AzA-treated mice, showing erythema and lesions in the AzA-treated group. (**d**) Skin lesion scores were significantly higher in AzA-treated mice (n = 6), with erythema and dryness being the primary contributors to the observed lesions. (**e, f**) Representative H&E-stained images of mouse skin after 5 days of AzA treatment (bar = 50 μm). **(g)** Epidermal thickness was not significantly different compared with control skin. **(h)** Scratching bouts were significantly increased after 5 days of repeated AzA treatment (n = 6). (**i, j**) RT-qPCR analysis of dorsal skin: *Trpv3* was upregulated, and *Tmem79* was downregulated. (**k**) Immunofluorescence staining for TRPV3 showing stronger signals in AzA-treated skin, abolished by TRPV3-blocking peptide (bar = 50 μm). (**l**) Quantification of TRPV3 fluorescence intensity confirmed AzA-induced upregulation and its suppression by blocking. * $P < .05$ and *** $P < .001$. Con denotes control. AzA, azelaic acid; ns, not significant.

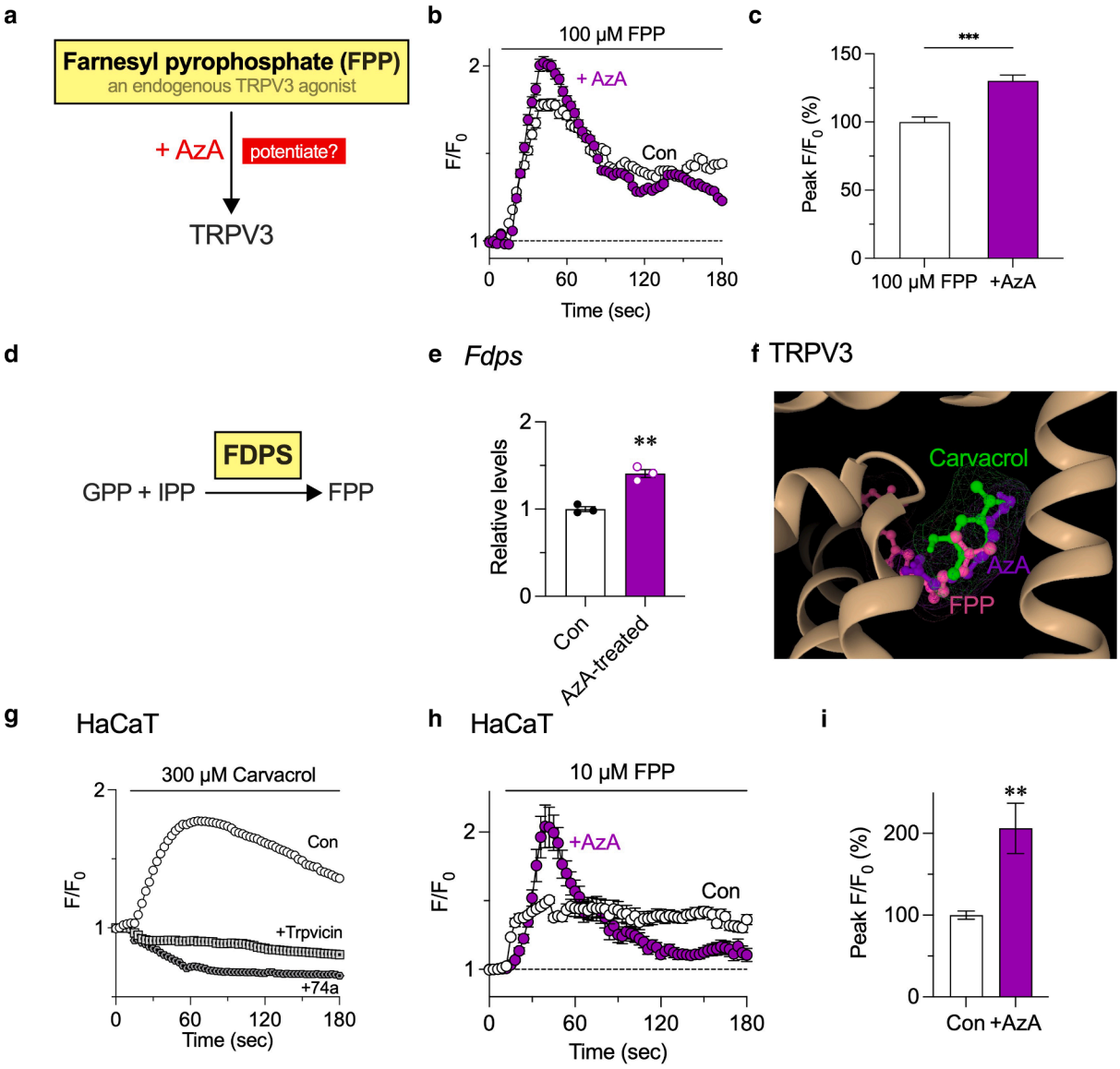

Supplementary Figure S4. (**a**) Schematic illustration of the hypothesis that AzA enhances TRPV3 activity by potentiating the endogenous TRPV3 agonist FPP. **(b)** Calcium imaging traces showing TRPV3 responses to 100 μM FPP with or without AzA. AzA pretreatment markedly enhanced FPP-induced calcium signaling. **(c)** Quantification of peak calcium responses confirming significant potentiation by AzA (n = 2726) compared with control (n = 2460). **(d)** Schematic of FPP biosynthesis from GPP and IPP through the enzyme FDPS. **(e)** RT-qPCR analysis showing increased *Fdps* expression in dorsal skin of AzA-treated mice. **(f)** Molecular docking model illustrating overlapping binding of FPP, AzA, and carvacrol in the similar region of TRPV3. **(g)** Calcium imaging traces from HaCaT cells show that both trpvicin and TRPV3-74a effectively suppress TRPV3 activation by carvacrol (300 μM), confirming the specificity of TRPV3-mediated responses in this cell line (+Trpvicin; n = 895, +Trpv3-74a; n = 1346) compared with the control (n = 508). (**h**) Calcium responses to 10 μM FPP were also potentiated by AzA pretreatment in HaCaT cells. (**i**) Quantification of peak FPP-induced responses showing significant enhancement by AzA (n = 68) compared with the control (n = 56). $^{**}P < .01$ and $^{***}P < .001$. AzA, azelaic acid; FDPS, farnesyl diphosphate synthase; FPP, farnesyl pyrophosphate; GPP, geranyl pyrophosphate; IPP, isopentenyl pyrophosphate; sec, second.